



Mohjazi, L., Bariah, L., Muhaidat, S., Sofotasios, P. C., Onireti, O. and Imran, M. (2019) Error Probability Analysis of Non-Orthogonal Multiple Access for Relaying Networks with Residual Hardware Impairments. In: 2019 IEEE 30th Annual International Symposium on Personal, Indoor and Mobile Radio Communications (PIMRC), Istanbul, Turkey, 08-11 Sep 2019, ISBN 9781538681107.

There may be differences between this version and the published version. You are advised to consult the publisher's version if you wish to cite from it.

<http://eprints.gla.ac.uk/188081/>

Deposited on: 27 June 2019

# Error Probability Analysis of Non-Orthogonal Multiple Access for Relaying Networks with Residual Hardware Impairments

Lina Mohjazi<sup>‡</sup>, Lina Bariah<sup>‡</sup>, Sami Muhaidat<sup>‡</sup>, Paschalis C. Sofotasios<sup>‡</sup>, Oluwakayode Onireti\*, and Muhammad Ali Imran\*

<sup>‡</sup>Center for Cyber-Physical Systems, Department of Electrical and Computer Engineering, Khalifa University, Abu Dhabi, UAE

(e-mail: {l.mohjazi, lina.bariah, muhaidat, p.sofotasios}@ieee.org)

\*School of Engineering, University of Glasgow, Glasgow, UK

(e-mail: {Oluwakayode.Onireti, Muhammad.Imran}@glasgow.ac.uk)

**Abstract**—In this paper, we quantify the effect of residual hardware impairments (RHI) on the error rate performance of a relay-based non-orthogonal multiple access (NOMA) system, where the communication between a source node and multiple users is completed via an amplify-and-forward (AF) relay node. In particular, we focus on the pairwise error probability (PEP) analysis and derive an accurate PEP approximation to characterize the performance of NOMA users under Rayleigh fading channels. The derived PEP expression is then exploited to investigate the diversity gain and the union bound on the bit error rate (BER) of the underlying system. Our results demonstrate that the presence of RHI causes an error floor at high signal-to-noise ratio (SNR) values. This error floor yields a detrimental effect on the achievable diversity order of NOMA users, where it is shown that the diversity order of all users converges to zero.

## I. INTRODUCTION

Non-orthogonal multiple access (NOMA) has been envisaged as a potential enabling technology for future wireless networks [1]. Based on the concept of superposing multiple users' signals through power domain multiplexing at the same resource block, such as time, frequency, or code. NOMA can scale up the system capacity and improve the spectral efficiency compared to existing orthogonal multiple access (OMA) schemes, such as, code division multiple access (CDMA), frequency division multiple access (FDMA), and time division multiple access (TDMA), [2]. In a NOMA system, less transmit power is allocated to users with stronger channel conditions and higher transmit power is allocated to users with weaker channel conditions. Consequently, a trade-off is realized between user fairness and system throughput. At the receiver end, successive interference cancellation (SIC) is adopted to decode the user-specific message and eliminate interference [3].

Among various research directions for NOMA, recently, its application in relaying networks was investigated to enhance the transmission reliability and extend the network coverage [2], [4]–[6]. A cooperative scheme for NOMA was first proposed in [2] for a cellular network with multiple users, where users with strong channel conditions act as relays to assist the users with weak channel conditions. The concept of NOMA was then

introduced for many scenarios. For example, the authors in [4] studied the performance of NOMA in simultaneous wireless information and power transfer (SWIPT) relaying networks. In [5], the authors investigated the application of NOMA in cognitive radio networks (CRNs). On the other hand, the research studies presented in [6] (and the references therein) considered the employment of a dedicated relay node to improve the performance of NOMA systems.

The overwhelming literature consider the ideal radio-frequency (RF) hardware assumption, which is rather unrealistic for practical applications. More specifically, in practice, wireless transceivers hardware may be corrupted by hardware imperfections such as, amplifier nonlinearities, in-phase/quadrature-phase (I/Q) imbalance, and oscillator phase noise, which are known to induce irrecoverable distortions in the transmitted and received signals [7]. These impairments are typically mitigated with the aid of either calibration techniques at the transmitter or compensation algorithms at the receiver, or both [7]. Nevertheless, these mechanisms fail to completely remove the hardware impairments due to a number of factors, such as imperfect parameter estimation, time variation of the hardware characteristics, the randomness induced by different types of noise, or imperfect compensation schemes. As a result, a certain amount of unaccounted for distortion always exists due to the residual hardware impairments (RHI), which are added to either the transmitted or received signal, or both [7].

Recently, the impact of RHI on the performance of relaying networks was investigated in [8], [9]. More recently, the authors in [10] presented a performance analysis framework to investigate the effect of RHI on the outage probability, ergodic sum rate, and individual sum rate of NOMA-based amplify-and-forward (AF) relaying systems, where RHI in all nodes is considered. It is widely known that user fairness is offered by NOMA, however, analyzing the individual reliability of each user in terms of error rate is essential to provide key insights into the quality-of-service (QoS) of weak and strong users. To the best of the authors' knowledge, none of previous works addressed the error probability performance analysis of

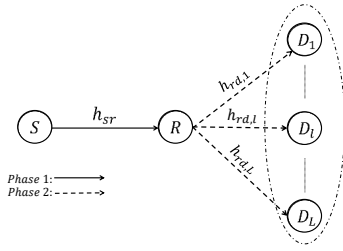


Figure 1: NOMA Downlink Relaying System

NOMA relaying systems suffering from RHI, which is the aim of this work.

In this work, we propose a mathematical framework to analyze the pairwise error probability (PEP) performance of NOMA-based AF relaying systems subject to RHI. PEP constitutes the stepping stone for the derivation of union bounds on the bit error rate (BER). It is widely used in literature to analyze the achievable diversity order and to provide useful insights into the error rate performance of each user, where closed-form BER expressions are intractable [11].

The rest of the paper is organized as follows. Sec. II presents the considered system and channel models. In Sec. III, a mathematical framework is developed to provide an accurate approximation of the PEP performance of NOMA users. Numerical and simulation results are discussed in Sec. IV and the conclusions are presented in Sec. V.

*Notation:* A circularly symmetric complex Gaussian random variable  $z$  with mean  $\mu$  and variance  $\sigma^2$  is given as  $z \sim \mathcal{CN}(\mu, \sigma^2)$ .  $\Re\{\cdot\}$  presents the real part of a complex number. Furthermore,  $x$ ,  $\hat{x}$ , and  $\tilde{x}$  denote the transmitted data symbol, detected data symbol, and incorrectly detected symbol, respectively. Also,  $x - \hat{x} \triangleq \hat{\Delta}$  and  $x - \tilde{x} \triangleq \tilde{\Delta}$ . Finally,  $(\cdot)^*$  and  $|\cdot|$  stand for the complex conjugate and the absolute value operations, respectively.

## II. SYSTEM MODEL

We consider a relay-based downlink NOMA scenario, as depicted in Fig. 1. In this setup, a source node,  $S$ , transmits mutually independent information to  $L$  users  $\{D_l\}_{l=1}^L$  simultaneously via an AF relay,  $R$ . We assume that all nodes are equipped with a single antenna and operate in a half-duplex mode. It is further assumed that the direct link is strongly attenuated, due to deep fading, shadowing, or blockages effects, and communication can be completed only through the relay node. Therefore, we consider that the direct link does not exist between  $S$  and the users  $\{D_l\}_{l=1}^L$ .

Moreover, for mathematical tractability, we consider a homogeneous network topology, where all users are located in a close proximity to each other. According to this setup, all channels between the relay and users are modeled as independent and identically distributed (i.i.d) Rayleigh fading channels [6]. The channel coefficients of the  $S \rightarrow R$  and the  $R \rightarrow D_l$  links are denoted by  $h_{sr} \sim \mathcal{CN}(0, \sigma_{sr}^2)$  and  $h_{rd,l} \sim \mathcal{CN}(0, \sigma_{rd,l}^2)$ , respectively. To simplify the subsequent analysis, we assume that  $\sigma_h^2 = \sigma_{sr}^2 = \sigma_{rd,l}^2$ . Without loss of generality and according to the respective channel gains of users, it is

assumed that they are sorted in an ascending order, i.e.  $|h_{rd,1}|^2 < \dots < |h_{rd,l}|^2 < \dots < |h_{rd,L}|^2$ . The concept of NOMA is applied by multiplexing different users in power domain, where each user is assigned a distinct power level. More specifically, high power values are allocated to users with weak channel conditions, while low power coefficients are allocated for users with strong channel conditions.

In this paper, we adopt the conventional AF scheme for NOMA downlink cooperative systems. In particular, the data transmission is completed over two phases. In *Phase-1* and given the total transmit power  $P_s$ , the source  $S$  transmits to  $R$  the superimposed signal given by

$$s = \sum_{l=1}^L \sqrt{\alpha_l P_s} x_l, \quad (1)$$

where  $x_l$  is the data symbol intended for the  $l$ -th user (i.e.,  $D_l$ ), and  $\alpha_l$  is the power allocation coefficient of the  $l$ -th user. Following the NOMA principal, we have  $\alpha_1 > \dots > \alpha_l > \dots > \alpha_L$  and  $\sum_{l=1}^L \alpha_l = 1$ .

As such, the signal received by the relay  $R$  characterizing the RHI can be expressed as

$$y_r = h_{sr} \left( \sum_{l=1}^L \sqrt{\alpha_l P_s} x_l + \eta_{sr} \right) + n_r, \quad (2)$$

where  $n_r \sim \mathcal{CN}(0, \sigma_n^2)$  denotes the additive white Gaussian noise (AWGN) at  $R$  and the independent distortion noise  $\eta_{sr} \sim \mathcal{CN}(0, \kappa_{sr}^2 P_s)$  denotes RHI at both the transmitter,  $S$ , and the receiver,  $R$ . Furthermore,  $\kappa_{sr} \triangleq \sqrt{\kappa_{s,t}^2 + \kappa_{r,r}^2}$  is the aggregate level of RHI of the  $S \rightarrow R$  link, where  $\kappa_{s,t}, \kappa_{r,r} \geq 0$  are the design parameters attributed to the level of hardware impairments in  $S$  and  $R$ , respectively [10]. The values of  $\kappa_{s,t}$  and  $\kappa_{r,r}$  are measured as error vector magnitudes (EVMs).

During *Phase-2*,  $R$  broadcasts  $y_r$  to all users after multiplying it with an amplifying gain

$$G = \sqrt{\frac{P_r}{(1 + \kappa_{sr}^2) P_s |h_{sr}|^2 + \sigma_{n,r}^2}}, \quad (3)$$

where  $P_r$  is the transmit power at  $R$ . Also, under RHI, the relay introduces additional distortion noise in the transmitted signal. Consequently, the signal received at  $D_l$  in the second phase is given by

$$\begin{aligned} y_{D_l} &= h_{rd,l} G \left[ h_{sr} \left( \sum_{l=1}^L \sqrt{\alpha_l P_s} x_l + \eta_{sr} \right) + n_r \right] \\ &\quad + h_{rd,l} \eta_{rd,l} + n_{D_l} \\ &= \underbrace{G h_{sr} h_{rd,l} \sum_{l=1}^L \sqrt{\alpha_l P_s} x_l}_{\text{Signal Part}} \\ &\quad + \underbrace{G h_{sr} h_{rd,l} \eta_{sr} + h_{rd,l} \eta_{rd,l}}_{\text{RHI Noise Part}} + \underbrace{G h_{rd,l} n_r + n_{D_l}}_{\text{AWGN Noise Part}}, \end{aligned} \quad (4)$$

where  $n_{D_l} \sim \mathcal{CN}(0, \sigma_n^2)$  denotes the AWGN and  $\eta_{rd,l} \sim \mathcal{CN}(0, \kappa_{rd,l}^2 P_r)$  is the aggregate distortion noise due to RHI of the  $R \rightarrow D_l$  link. Furthermore,  $\kappa_{rd,l} = \sqrt{\kappa_{r,t}^2 + \kappa_{D_l,r}^2}$ , where  $\kappa_{r,t}$  and  $\kappa_{D_l,r}$  denote the levels

$$\Pr\left(x_l \rightarrow \tilde{x}_l \mid h_{sr}h_{rd,l}\right) = \Pr\left(\left|Gh_{sr}h_{rd,l}\beta_l + Gh_{sr}h_{rd,l}\eta_{sr} + Gh_{rd,l}n_r + h_{rd,l}\eta_{rd,l} + n_{D_l}\right|^2 \leq \left|Gh_{sr}h_{rd,l} \sum_{i=l+1}^L \sqrt{\alpha_i P_s} x_i + Gh_{sr}h_{rd,l}\eta_{sr} + Gh_{rd,l}n_r + h_{rd,l}\eta_{rd,l} + n_{D_l}\right|^2\right). \quad (7)$$

of hardware impairments in  $R$  and  $D_l$ , respectively. Following [8], [10], we assume that the impairment levels of users are the same, i.e.,  $\kappa_{D,r}^2 = \kappa_{D_l,r}^2$ . Therefore,

$$\kappa_{rd} \triangleq \kappa_{rd,l} = \sqrt{\kappa_{r,t}^2 + \kappa_{D,r}^2}.$$

By performing SIC at each user to separate the superimposed symbols and mitigate the inter-user interference, reliable detection for the intended user's message is achieved. To this end, users with better channel conditions decode the signals intended for other users prior to decoding their own, such that, the optimal order for SIC is achieved on the basis of increasing channel gain. Therefore,  $D_l$  first detects the signals of  $D_i, i < l$  before decoding its own signal. Moreover, the signals corresponding to the rest of the users, i.e.,  $D_i, i > l$ , will be treated as interference. The SIC technique will be implemented in a successive manner until  $l$  users' messages are all decoded [3].

Accordingly, the output of the SIC at the  $l$ -th user receiver is expressed as

$$y'_{D_l} = \left( \sqrt{\alpha_l P_s} x_l + \sum_{i=1}^{l-1} \sqrt{\alpha_i P_s} \hat{\Delta}_i + \sum_{i=l+1}^L \sqrt{\alpha_i P_s} x_i \right) \times Gh_{sr}h_{rd,l} + Gh_{sr}h_{rd,l}\eta_{sr} + h_{rd,l}\eta_{rd,l} + Gh_{rd,l}n_r + n_{D_l}, \quad (5)$$

where  $\sum_{i=1}^{l-1} \sqrt{\alpha_i P_s} \hat{\Delta}_i$  describes the interference resulting from performing SIC for users  $D_1, \dots, D_{l-1}$ ,  $\hat{\Delta}_i = x_i - \tilde{x}_i$ , while  $\sum_{i=l+1}^L \sqrt{\alpha_i P_s} x_i$  denotes the interfering signals due to users  $D_{l+1}, \dots, D_L$ .

### III. PAIRWISE ERROR PROBABILITY ANALYSIS

In this section, we derive the PEP expression for the  $l$ -th NOMA user. This expression will then be employed to evaluate the union bound of the BER.

#### A. PEP Analysis of the $l$ -th User

PEP is defined as the probability of detecting symbol  $\tilde{x}$  given that symbol  $x$  was transmitted. Accordingly, the conditional PEP of the  $l$ -th user can be evaluated as

$$\Pr(x_l \rightarrow \tilde{x}_l \mid h_{sr}h_{rd,l}) = \Pr\left(\left|y'_{D_l} - \sqrt{\alpha_l P_s} Gh_{sr}h_{rd,l} \tilde{x}_l\right|^2 \leq \left|y'_{D_l} - \sqrt{\alpha_l P_s} Gh_{sr}h_{rd,l} x_l\right|^2\right), \quad (6)$$

where  $\tilde{x} \neq x$ . By expanding (6), the conditional PEP of the  $l$ -th user can be expressed as (7), given at the top of this page, where  $\beta_l$  is expressed as

$$\beta_l = \sqrt{\alpha_l P_s} \tilde{\Delta}_l + \sum_{i=1}^{l-1} \sqrt{\alpha_i P_s} \hat{\Delta}_i + \sum_{i=l+1}^L \sqrt{\alpha_i P_s} x_i, \quad (8)$$

such that  $\tilde{\Delta}_l = x_l - \tilde{x}_l$ . It is recalled that, in order for the  $l$ -th user to detect its own signal, the signals of the users with lower detection order, i.e.  $x_1, \dots, x_{l-1}$ , are first detected and subtracted. As a consequence, the residual interference from  $x_{l+1}, \dots, x_L$  becomes less significant and can be considered as additive noise [11].

By further expanding (7), it can be rewritten as (9), given at the top of the next page, where  $\omega_1 = |h_{sr}|$  and  $\omega_{2,l} = |h_{rd,l}|$ . It is noted that the real part of the Gaussian noise in (9) is normally distributed with zero mean and  $\sigma_n^2/2$  variance, and the decision variable in (9) is Gaussian and can be expressed as (10), given at the top of the next page. Recalling that, for  $\Lambda \sim \mathcal{N}(\mu, \sigma^2)$  [12]

$$\Pr(\Lambda \leq \lambda) = Q\left(\frac{\lambda - \mu}{\sigma}\right), \quad (11)$$

the conditional PEP is given by (12), at the top of the next page, where  $Q(x) = \frac{1}{\sqrt{2\pi}} \int_x^\infty \exp(-u^2/2) du$  is the Gaussian Q-function [12]. By substituting (3) in (12) and rewriting the Q-function in terms of the complementary error function, i.e.  $Q(x) = \frac{1}{2} \operatorname{erfc}\left(\frac{x}{\sqrt{2}}\right)$ , (12) can be expressed as

$$\Pr\left(x_l \rightarrow \tilde{x}_l \mid \omega_1 \omega_{2,l}\right) = \frac{1}{2} \operatorname{erfc}\left(\frac{\sqrt{P_r} \omega_1 \omega_{2,l} \Psi}{2|\tilde{\Delta}_l|^2 \sqrt{\omega_1^2 \left(\omega_{2,l}^2 \xi + \bar{\kappa}_{sr}^2 P_s \sigma_n^2\right) + \omega_{2,l}^2 \zeta + \sigma_n^2}}\right). \quad (13)$$

where  $\bar{\kappa}_{sr}^2 = (1 + \kappa_{sr}^2)$ ,  $\xi = \kappa_{sr}^2 P_s P_r + \bar{\kappa}_{sr}^2 \kappa_{rd,l}^2 P_s P_r$ , and  $\zeta = P_r \sigma_n^2 + \kappa_{rd,l}^2 P_r \sigma_n^2$ . By noting that  $\omega_1$  follows the Rayleigh distribution, the exact PEP of the  $l$ -th user, conditioned on the random variable (RV)  $\omega_{2,l}$ , can be evaluated by averaging (13) over the probability density function (PDF) of  $\omega_1$  yielding the expression in (14), given at the top of the next page. Note that, deriving an exact closed-form expression for (14) is mathematically intractable. However, this can be treated by resorting to the Gauss-Laguerre Quadrature (GLQ) method [13] to efficiently and accurately approximate the integral in (14) as (15) given at the top of page 5, where  $\delta_m$  and  $x_m$  are the  $m$ -th weight and root, respectively, of the  $m$ -th order Laguerre polynomial (tabulated in [13]). Also in (15),  $M$  determines the accuracy of the numerical evaluation.

$$\begin{aligned}
& \Pr\left(x_l \rightarrow \tilde{x}_l \mid h_{sr} h_{rd,l}\right) = \\
& \Pr\left(\underbrace{2\Re\left\{G^2\omega_1\omega_{2,l}\sqrt{\alpha_l P_s}\tilde{\Delta}_l\eta_{sr}^* + G^2\omega_{2,l}^2 h_{sr}\sqrt{\alpha_l P_s}\tilde{\Delta}_l n_r^* + G\omega_{2,l}h_{sr}\sqrt{\alpha_l P_s}\tilde{\Delta}_l\eta_{rd,l}^* + Gh_{sr}h_{rd,l}\sqrt{\alpha_l P_s}n_{D_l}^*\right\}}_N\right. \\
& \quad \left.\leq -G^2\omega_1\omega_{2,l}\left(\underbrace{|\beta_l|^2 - \left|\sum_{i=1}^{l-1}\sqrt{\alpha_i P_s}\hat{\Delta}_i + \sum_{i=l+1}^L\sqrt{\alpha_i P_s}x_i\right|^2}_{\Psi}\right)\right). \tag{9}
\end{aligned}$$

$$N \sim \mathcal{N}\left(0, 2G^2\alpha_l P_s |\tilde{\Delta}_l|^2 \omega_1^2 \omega_{2,l}^2 \left[G^2\omega_1^2 \omega_{2,l}^2 \kappa_{sr}^2 P_s + G^2\omega_{2,l}^2 \sigma_n^2 + \omega_{2,l}^2 \kappa_{rd,l}^2 P_r + \sigma_n^2\right]\right) \tag{10}$$

$$\Pr\left(x_l \rightarrow \tilde{x}_l \mid \omega_1\omega_{2,l}\right) = Q\left(\frac{G\omega_1\omega_{2,l}\Psi}{|\tilde{\Delta}_l|\sqrt{2\alpha_l P_s}\sqrt{G^2\omega_1^2 \omega_{2,l}^2 \kappa_{sr}^2 P_s + G^2\omega_{2,l}^2 \sigma_n^2 + \omega_{2,l}^2 \kappa_{rd,l}^2 P_r + \sigma_n^2}}\right). \tag{12}$$

$$\Pr\left(x_l \rightarrow \tilde{x}_l \mid \omega_{2,l}\right) = \frac{1}{2\sigma_h^2} \int_0^\infty x \exp\left(\frac{-x^2}{2\sigma_h^2}\right) \operatorname{erfc}\left(\frac{\sqrt{P_r}\omega_{2,l}\Psi x}{2|\tilde{\Delta}_l|^2\sqrt{x^2\left(\omega_{2,l}^2\xi + \bar{\kappa}_{sr}^2 P_s \sigma_n^2\right) + \omega_{2,l}^2\zeta + \sigma_n^4}}\right) dx. \tag{14}$$

To evaluate the unconditional PEP, the conditional PEP in (15) is averaged over the PDF of  $\omega_{2,l}$ . It is recalled that the first user always has the weakest channel, and that the channel gains for the remaining users are ordered in ascending order. The ordered PDF of the channel gain of the  $l$ -th user, can be represented based on the order statistics theory as [12]

$$f_{\omega_{2,l}}(y) = A_l f_Y(y) [F_Y(y)]^{l-1} [1 - F_Y(y_{2,l})]^{L-l}, \tag{16}$$

where  $A_l = L!/((l-1)!(L-l)!)$ . Considering that  $|h_{rd,l}|$  is Rayleigh distributed, using (16), the PDF of  $|h_{rd,l}| \triangleq \omega_{2,l}$  is given by [11]

$$f_{\omega_{2,l}}(y) = \frac{A_l y}{\sigma_h^2} \sum_{j=0}^{l-1} \binom{l-1}{j} (-1)^j \exp\left(-\frac{(L-l+j+1)y^2}{2\sigma_h^2}\right). \tag{17}$$

Therefore, by averaging (15) over (17), the unconditional PEP can be given as (18), in the next page. To the best of our knowledge, the integral in (18) does not lend itself to a closed-form, however, we apply the GLQ rule to provide an accurate approximation of (18) as (19), given at the top of the next page. In (19), where  $\delta_z$  and  $y_z$  are the  $z$ -th weight and root, respectively, of the  $z$ -th order Laguerre polynomial (tabulated in [13]). Also,  $Z$  determines the accuracy of the numerical evaluation.

## B. BER Union Bound

It is widely stated in the literature of NOMA-based systems that deriving the exact BER in a closed-form is challenging, since it is dependent on the applied channel coding or modulation schemes. Additionally, the effect of error propagation due to imperfect SIC yields the analysis of exact BER in NOMA to be mathematically intractable [2], [4], [5], [10]. In this context, the motivation of analyzing the PEP performance in NOMA is also manifested in facilitating a tractable mathematical framework [11]. As such, useful insights about the error rate performance of NOMA users, under different fading scenarios can be provided by exploiting the PEP analysis and the corresponding BER union bound. Therefore, using the PEP expression given in (19), the BER union bound can be evaluated using [12]

$$P_e \leq \frac{1}{n} \sum_{x_l} \Pr(x_l) \sum_{x_l \neq \hat{x}_l} \Pr\left(x_l \rightarrow \hat{x}_l \mid x_l, \hat{\Delta}_l\right) \times q(x_l \rightarrow \hat{x}_l), \quad \forall i \neq l, \tag{20}$$

where  $n$  is the number of information bits in symbol  $x_l$ ,  $\Pr(x_l)$  denotes the probability of transmitting symbol  $x_l$  and  $q(x_l \rightarrow \hat{x}_l)$  is the number of bit errors when  $x_l$  is transmitted and  $\hat{x}_l$  is detected. Also,  $\Pr\left(x_l \rightarrow \hat{x}_l \mid x_l, \hat{\Delta}_l\right)$  represents the conditional PEP. Therefore, the average

$$\Pr\left(x_l \rightarrow \tilde{x}_l \mid \omega_{2,l}\right) \approx \frac{1}{2\sigma_h^2} \sum_{m=1}^M \delta_m \exp(x_m) \exp\left(\frac{-x_m^2}{2\sigma_h^2}\right) \operatorname{erfc}\left(\frac{\sqrt{P_r} \omega_{2,l} \Psi x_m}{2|\tilde{\Delta}_l|^2 \sqrt{x_m^2 (\omega_{2,l}^2 \xi + \bar{\kappa}_{sr}^2 P_s \sigma_n^2) + \omega_{2,l}^2 \zeta + \sigma_n^4}}\right). \quad (15)$$

$$\Pr\left(x_l \rightarrow \tilde{x}_l\right) \approx \frac{A_l}{2\sigma_h^4} \sum_{m=1}^M \sum_{j=0}^{l-1} \binom{l-1}{j} (-1)^j \delta_m \exp\left(\frac{-x_m^2}{2\sigma_h^2} + x_m\right) \left[ \int_0^\infty y \exp\left(\frac{-(L-l+j+1)y^2}{2\sigma_h^2}\right) \times \operatorname{erfc}\left(\frac{\sqrt{P_r} \Psi x_m y}{2|\tilde{\Delta}_l|^2 \sqrt{x_m^2 (y^2 \xi + \bar{\kappa}_{sr}^2 P_s \sigma_n^2) + y^2 \zeta + \sigma_n^4}}\right) dy \right]. \quad (18)$$

$$\Pr\left(x_l \rightarrow \tilde{x}_l\right) \approx \frac{A_l}{2\sigma_h^4} \sum_{m=1}^M \sum_{z=1}^Z \sum_{j=0}^{l-1} \binom{l-1}{j} (-1)^j \delta_m \delta_z \exp\left(\frac{-x_m^2}{2\sigma_h^2} + x_m\right) \exp\left(\frac{-(L-l+j+1)y_z^2}{2\sigma_h^2} + y_z\right) \times \operatorname{erfc}\left(\frac{\sqrt{P_r} \Psi x_m y_z}{2|\tilde{\Delta}_l|^2 \sqrt{x_m^2 (y_z^2 \xi + \bar{\kappa}_{sr}^2 P_s \sigma_n^2) + y_z^2 \zeta + \sigma_n^4}}\right). \quad (19)$$

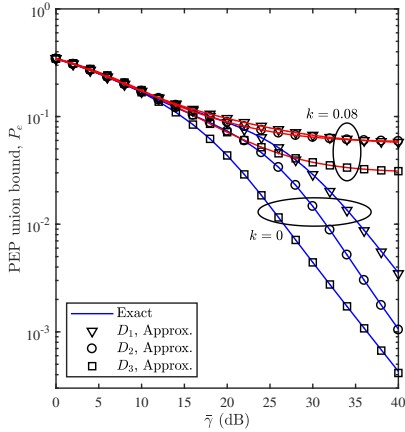


Figure 2: Analytical and simulated exact BER union bound for different users vs. the average SNR,  $\bar{\gamma}$ ,  $\kappa = 0, 0.08$ .

BER union bound can be evaluated by averaging over all possible scenarios of  $x_l$ ,  $\hat{x}_l$ , and  $\hat{\Delta}$ .

#### IV. NUMERICAL AND SIMULATION RESULTS

In this section, we present a set of numerical and Monte Carlo simulations to validate the derived theoretical results and to examine the error rate performance of a NOMA relaying system impaired with RHI under various scenarios. In the adopted NOMA system, we consider the case of three users, i.e.,  $L = 3$ . The link between the source node and the relay node and that between the relay node and each user are modeled as flat fading channels with Rayleigh PDF. It is worth mentioning that these fading channels are generated randomly and then ordered and assigned to users based on their order. Specifically, the three generated Rayleigh random variables are assigned as follows. The weakest is assigned to the first user and

the strongest is assigned to the third user. Simulation results are obtained by performing  $10^5$  channel realizations. Moreover, the transmitted and detected signals are chosen randomly from binary phase shift keying (BPSK) constellation.

In our simulations and without loss of generality, we assume that  $P \triangleq P_s = P_r$ , where  $P$  is set to unity. Furthermore, in our results, we refer to  $\bar{\gamma} = P/\sigma_n^2$  as the average system signal to noise (SNR) ratio. Unless otherwise mentioned, the power allocation coefficients are chosen as  $\alpha_1 = 0.7$ ,  $\alpha_2 = 0.2$ , and  $\alpha_3 = 0.1$ . Following the assumption in [10], we consider that the  $S \rightarrow R$  and  $R \rightarrow D_l$  links exhibit the same impairment level, i.e.,  $\kappa \triangleq \kappa_{sr} = \kappa_{rd,l}$ . Additionally, in computing the generalized GLQ approximations, we choose  $M = Z = 60$ .

Fig. 2 compares the exact and approximated BER union bound of the impaired users,  $\kappa = 0.08$ , with the ideal case,  $\kappa = 0$ . The approximated analytical union bound is given in (20) and (19) while the exact union bound results are generated using Monte Carlo simulations. From the figure, it can be observed that the analytical union bound perfectly matches the exact union bound over the entire SNR range. This implies that the adopted GLQ method yields an accurate solution to the integrals in (14) and (18), which validates the accuracy of the PEP expression in (19). Furthermore, as shown in Fig. 2, the error rate performance of NOMA users is highly susceptible to the existence of RHI. In specific, it can be noticed that the BER union bound of all users experiences an error floor when  $\kappa = 0.08$ , and this error floor occurs at high SNR values,  $\bar{\gamma} > 20$  dB. It is worth noting that similar conclusions can be obtained for higher  $\kappa$  values, however, results obtained for different  $\kappa$  values are omitted for clarity.

The achievable diversity order of NOMA users under

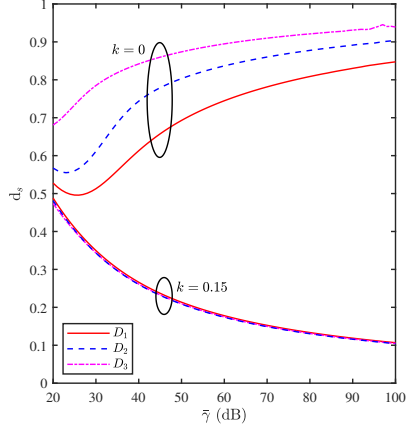


Figure 3: Diversity gain for users  $l = 1, 2$  and  $3$ , vs. the average SNR,  $\bar{\gamma}$ ,  $\kappa = 0, 0.15$ .

RHI scenario is investigated in Fig. 3, which is defined as the slope of the BER union bound when the SNR approaches infinity. The presented results in Fig. 3 capture the effect of RHI on the error rate performance of NOMA users, where it is observed that the diversity order of all users approaches zero at high SNR values, when  $\kappa = 0.15$ . This diversity order loss is a consequence of the observed error floor that happens at high SNR values. It is recalled that, regardless of users' order, the achievable diversity order of NOMA users in the ideal case approaches unity, due to the utilization of single relay.

The effect of the RHI level,  $\kappa$ , on the error rate performance is demonstrated in Fig. 4, for different SNR values,  $\bar{\gamma} = 20$  and  $35$  dB. It is worth noting that the practical values of  $\kappa$  fall in the range  $[0.08, 0.175]$  [7]. It can be observed from Fig. 4 that for lower SNR values,  $\bar{\gamma} = 20$  dB, increasing the impairment level,  $\kappa$ , has negligible effect on the BER union bound performance of all users, which verifies that the RHI introduces a performance loss at high SNR values. Emphasizing on this, it can be noticed from Fig. 4 that at higher SNR values,  $\bar{\gamma} = 35$  dB, the error rate encounters high performance degradation as the  $\kappa$  value increases. Moreover, it can be noticed that the effect of increasing the RHI level is more notable on higher order users, and this is can be justified by the effect of the imperfect SIC process. In specific, due to the RHI, the probability of successful SIC process deteriorates, hence causing an increased interference from users with higher power levels. Recalling that the first user does not perform SIC, the first user is less vulnerable to increasing  $\kappa$  values. For example, when the value of  $\kappa$  increases from  $0.05$  to  $0.1$ , the BER union bound performance degradation of the third user is approximately equal to  $8.7$  dB, whereas for the first user, the performance degradation is approximately equal to  $5.7$  dB.

## V. CONCLUSIONS

This paper provided an analytical framework to investigate the impact of RHI on a NOMA-based relaying network. An accurate and efficient approximation of the PEP is obtained to examine the union bound of the average BER of the considered system. Specifically our results illustrated that RHI has a high impact on the

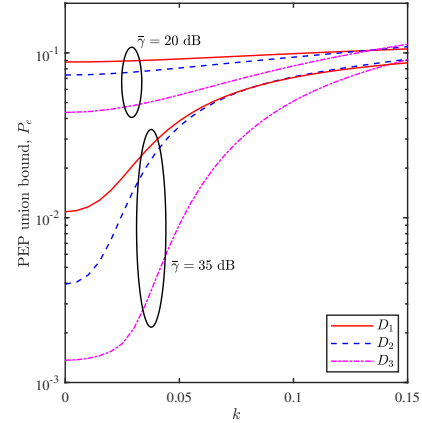


Figure 4: BER union bound for different users vs. the RHI level,  $\kappa$ ,  $\bar{\gamma} = 20$  and  $35$  dB.

error rate performance, where for practical RHI levels, the achievable diversity order of NOMA users approaches zero. This diversity order degradation is induced by the error floor experienced by NOMA users at high SNR values under RHI. Moreover, due to the effect of imperfect SIC process, higher order users are more susceptible to higher levels of RHI.

## REFERENCES

- [1] W. Shin, M. Vaezi, B. Lee, D. J. Love, J. Lee, and H. V. Poor, "Non-Orthogonal multiple access in multi-cell networks: Theory, performance, and practical challenges," *IEEE Commun. Mag.*, vol. 55, no. 10, pp. 176–183, Oct. 2017.
- [2] Z. Ding, M. Peng, and H. V. Poor, "Cooperative non-orthogonal multiple access in 5G systems," *IEEE Commun. Lett.*, vol. 19, no. 8, pp. 1462–1465, Aug. 2015.
- [3] Z. Ding, Y. Liu, J. Choi, Q. Sun, M. Elkashlan, C. I, and H. V. Poor, "Application of non-orthogonal multiple access in LTE and 5G networks," *IEEE Commun. Mag.*, vol. 55, no. 2, pp. 185–191, Feb. 2017.
- [4] T. Q. D. Nhu Tri Do, Daniel Benevides Da Costa and B. An, "A BNBF user selection scheme for NOMA-based cooperative relaying systems with SWIPT," *IEEE Commun. Lett.*, vol. 21, no. 3, pp. 664–667, Mar. 2017.
- [5] L. Lv, Q. Ni, Z. Ding, and J. Chen, "Application of non-orthogonal multiple access in cooperative spectrum-sharing networks over Nakagami- $m$  fading channels," *IEEE Trans. Vehic. Technol.*, vol. 66, no. 6, pp. 5506–5511, June 2017.
- [6] J. Men, J. Ge, and C. Zhang, "Performance analysis of nonorthogonal multiple access for relaying networks over Nakagami- $m$  fading channels," *IEEE Trans. Vehic. Technol.*, vol. 66, no. 2, pp. 1200–1208, 2017.
- [7] T. Schenk, *RF imperfections in high-rate wireless systems: impact and digital compensation*. Springer Science & Business Media, 2008.
- [8] P. K. Sharma and P. K. Upadhyay, "Cognitive relaying with transceiver hardware impairments under interference constraints," *IEEE Commun. Lett.*, vol. 20, no. 4, pp. 820–823, Apr. 2016.
- [9] B. Selim, S. Muhaidat, P. C. Sofotasios, B. S. Sharif, T. Stouraitis, G. K. Karagiannidis, and N. Al-Dhahir, "Performance analysis of non-orthogonal multiple access under I/Q imbalance," *IEEE Access*, vol. 6, pp. 18453–18468, 2018.
- [10] F. Ding, H. Wang, S. Zhang, and M. Dai, "Impact of residual hardware impairments on non-orthogonal multiple access based amplify-and-forward relaying networks," *IEEE Access*, vol. 6, pp. 15 117–15 131, 2018.
- [11] L. Bariah, S. Muhaidat, and A. Al-Dweik, "Error probability analysis of non-orthogonal multiple access over Nakagami- $m$  fading channels," *IEEE Trans. Commun.*, vol. 67, no. 2, pp. 1586–1599, Feb. 2019.
- [12] J. G. Proakis, *Digital Communications*. New York: McGraw-Hill, 4th edition, 2000.
- [13] P. Concus, D. Cassatt, G. Jaehnig, and E. Melby, "Tables for the evaluation of  $\int_0^\infty x^\beta e^{-x} f(x) dx$  by Gauss-Laguerre Quadrature," *Mathematics of Computation*, vol. 17, no. 83, pp. 245–256, 1963.